PHYSICAL REVIEW B VOLUME 19, NUMBER 8 15 APRIL 1979

Luminescence from pure MnF_2 and from MnF_2 doped with Eu^{3+} and Er^{3+}

B. A. Wilson* and W. M. Yen
Department of Physics, University of Wisconsin, Madison, Wisconsin 53706

J. Hegarty† and G. F. Imbusch
Department of Physics, University College, Galway, Ireland
(Received 10 October 1978)

In this paper we report fluorescence measurements made over a range of temperatures on nominally pure and on Er- and Eu-doped MnF_2. By studying the weak intrinsic fluorescence in nominally pure samples we can draw some conclusions about exciton decay and energy-transfer processes. The decay rate of the $E1$ excitons is dominated by transfer to traps and depends strongly on temperature, exhibiting an activation behavior proceeding through a higher-$E2$ state. In the rare-earth-doped crystals the optical excitation energy is shared between the Mn traps and the rare-earth ions. As the temperature is raised the excitation is redistributed between the rare-earth ions and the effective Mn traps leading to a temperature-dependent variation in the fluorescence spectra from these crystals.

I. INTRODUCTION

In this paper we examine the fluorescence properties of nominally pure MnF_2 and of MnF_2 doped with trace amounts of Eu and Er. The motivation for this study was to gain a better understanding both of the spectroscopy of the rare-earth-doped crystals and of the processes which affect the exciton annihilation and transfer in the MnF_2 system.

When Mn ions in MnF_2 are excited by the absorption of light into the higher absorption bands, the excited ions rapidly relax to the lowest excited $^4T_1$ level. Here the radiative lifetime is about 30 msec; this is a metastable level. Because of the strong interaction between adjacent Mn ions, this excitation does not stay on the same ion but can travel readily through the lattice of in-resonance Mn ions.[1,2] The correct description of such excited states is an exciton description.[3]

The combination of orthohombic crystal field, spin-orbit coupling, and exchange splits up the $^4T_1$ excited state of each Mn ion. The two lowest levels are labeled $E1$ and $E2$, 17 cm^{-1} apart, of which $E1$ is the lower.[3] $E1$ is the only level which can maintain a sizable population at low temperatures and the excitation transfer occurs through the $E1$ exciton states.

Even in the purest MnF_2 crystals, the fluorescence is associated mainly with impurities and/or defects.[1] Common impurities are Mg, Zn, and Ca ions which are inevitably present at concentrations of a few parts per million in these crystals. These impurities enter substitutionally for Mn ions, and they perturb the adjacent Mn ions, lowering the energy of their $E1$ levels below that of the regular Mn ions. The $E1$ excitons can become trapped at these perturbed Mn ions and at low temperatures this excitation cannot be returned to the $E1$ exciton state. Eventually these excited perturbed Mn ions decay radiatively with a fluorescence spectrum which is characteristic of the particular trap. The following common traps have been identified by means of the sharp pure electronic transitions from these depressed $E1$ levels which occur in addition to the much stronger magnon-assisted and phonon-assisted sidebands[1,2]: Mg(3nn) and Mg(2nn) traps, which are, respectively, Mn ions in third- and second-nearest-neighbor (nn) sites around Mg ions, and whose $E1$ levels are depressed by 48 and 77 cm^{-1}, respectively,[4] and Zn(3nn) and Zn(2nn) traps, which are, respectively, Mn ions in third- and second-nearest-neighbor sites around Zn ions, which have their $E1$ levels depressed by 36 and 66 cm^{-1}. Ca(1nn) traps are Mn ions in first-nearest-neighbor sites around Ca ions, and their $E1$ level is about 300 cm^{-1} below that of the regular Mn ions. In addition there is evidence for deeper Mn traps, about 1600 cm^{-1} below the regular $E1$ level,[5,6] whose nature is not yet clear. There is also the possibility that other 300-cm^{-1}-deep Mn traps can occur which do not exhibit sharp pure electronic transitions but only emit in the sidebands. Such, for example, might be Mg(1nn) and Zn(1nn) traps.

The absence of any fluorescence from these traps, however, may be explained with some success by comparing the radial strains produced by the impurities to the effects of uniaxial stress as measured by Dietz *et al.*[24] Since the ionic radii of Mg^{2+} and Zn^{2+} are smaller than that of Mn^{2+} the neighboring F^- ligands may move closer to the impurity, leading to a radial-type dilation. It has

been suggested[25] that a dilation along the c axis of MnF_2 will be compensated by a contraction in an orthogonal direction, and vice versa. Hence the 1nn Mn ions which lie along the c axis from the impurity will see a dilation along the c axis with a consequent contraction of its neighbors in the x-y plane. This effect is also achieved by applying uniaxial stress in the x-y plane which is found to perturb only weakly the energy of the $E1$ state.[24] Mg(1nn) and Zn(1nn), therefore, may not be deep enough to effectively trap the Mn excitation at the temperatures in question. Ca^{2+}, on the other hand, is larger than Mn^{2+}, giving rise to a radial compression of the F^- ligands. The effects of this for the 1nn Mn ion are similar to a [001] stress which strongly effects the $E1$ level, leading to very deep Ca(1nn) traps.

In the case of the 3nn Mn ions which lie in the x-y plane, the radial dilation caused by the presence of Mg or Zn is equivalent to a [001] stress which, as seen, greatly perturbs the $E1$ levels so these 2nn ions may be deep enough to trap the excitation at low temperatures. By the same line of argument Ca(3nn) ions may be too shallow to act as traps.

The situation with the 2nn Mn ions is more complex due to mixing of different strains, but they appear to follow the trend of the 3nn Mn ions.

All of the Mn traps are effective at low temperatures. At around 4 K, however, the shallower third-nearest-neightbor traps have begun to lose their trapped energy by boil back to the $E1$ exciton states through which it is conveyed to other deeper traps. Between 8 and 10 K, the second-nearest-neighbor traps lose their energy by boil back, and only the first-nearest-neighbor traps and deeper traps are operative.[1]

The loss of effectiveness of the second-nearest-neighbor traps is seen as a detectable (to the eye) shift in the color of the fluorescence from a yellow to a more orange color—due to the shift of the excitation energy to the lower fluorescent levels of the remaining effective traps. Careful photoelectric measurements, however, show little reduction in the integrated fluorescence intensity, indicating that in our crystals almost all of the excitation boiled off from the second-nearest-neighbor traps goes to the deeper traps and little is lost by nonradiative decay processes or by transfer to quenching traps.

As the temperature is raised still higher, above around 30 K, the deep Mn traps begin to lose their excitation by boil back and only the very deep quenching traps (probably Ni and Fe ions) remain.[2] The excitation eventually ends up on these traps from which it is either emitted as infrared radiation or lost nonradiatively. In either case it is not emitted as visible fluorescence; it is said to be quenched.

The fluorescence of the MnF_2 system, then, is characterized by traps. The radiative decay time of the Mn ions is so long that essentially all the excitation is transferred to traps, even though the Zn, Mg, and Ca ions which seem to be responsible for most of the traps are present in very small amounts—less than 100 ppm in these carefully grown crystals. Some very weak fluorescence due to the radiative decay of the pure $E1$ excitons is observed at low temperatures.[17] This consists of a sharp pure electronic transition between the $E1$ level of the regular Mn ions and the lowest ground-state level (this is called the $E1$ line and it occurs at 18423 cm^{-1}), its magnon sideband σ_1^*, and its phonon sideband farther to the red. Our ability to detect this fluorescence greatly assists the analysis of exciton decay processes in MnF_2, and we report on our studies of this intrinsic fluorescence in this paper.

Because of the efficient transfer to traps in these crystals, the notion of growing MnF_2 crystals with some rare-earth ions suggested itself—presumably the rare-earth ions would be efficiently excited by transfer from the $E1$ exciton system. Fluorescences from Eu^{3+} in[7,8] MnF_2 and[9,10] $KMnF_3$ from Er^{3+} in MnF_2,[5,11] and from Nd^{3+} in $RbMnF_3$[6,12] have been observed and analyzed.

In this study we examine the fluorescence from MnF_2:Eu, and MnF_2:Er and from nominally pure MnF_2 over a range of temperatures using broadband pumping as well as excitation by tunable pulsed dye lasers. In Sec. II we describe the materials studied and the experimental techniques used. Then we discuss the spectroscopy of the Eu^{3+} and Er^{3+} ions in MnF_2. Following this we describe our experiments on the exciton decay and energy-transfer processes in pure MnF_2 and in the rare-earth-doped crystals. In Sec. IV we attempt to relate the fluorescence properties of all these materials to each other in a consistent way.

II. MATERIALS AND EXPERIMENTAL TECHNIQUES

Crystals of nominally pure MnF_2 and of MnF_2 doped with Eu and Er were obtained from a number of sources. The one sample of MnF_2:Eu contained a nominal Eu concentration of 0.05 at.%. Neutron activation analysis, however, indicated an actual concentration of only 10^{-3} at.%, or 10 ppm. The three samples of MnF_2:Er were also analyzed by neutron activation. The nominally 0.2-at.% sample was found to have an Er concentration of 4×10^{-2} at.% (400 ppm). The concentration of Er in the two other MnF_2:Er samples were too low to be

measured by this method. Optical methods, however, yielded a ratio of Er concentrations of 1:6:150 for the nominally 0.05-, 0.1-, and 0.2-at.% samples, respectively, indicating that the nominally 0.1-at.% sample contained 1.6×10^{-3} at.% (16 ppm) and the nominally 0.05-at.% sample only 2.7×10^{-4} at.% (2.7 ppm). All samples were cut into the form of small rectangular prisms with the c axis parallel to one of the edges to facilitate polarization studies.

We find very small Eu and Er dopings in our samples, much less than the amount in the original mixture. We attribute the unusually small dopant levels in our crystals to the difficulty of incorporating the larger Eu^{3+} and Er^{3+} ions into the MnF_2 crystals. In particular, this seems to be the case when a second ion species is not included for charge compensation and when the crystals are carefully grown and slowly cooled, as in our case.

Sample temperatures below 4.2 K were achieved by immersing the sample in a bath of liquid helium. Temperatures above 4.2 K were achieved using either a temperature-controlled cold-finger cryostat or a helium-gas exchange cryostat. Temperatures in the 77–100-K region were obtained by blowing cold nitrogen gas over the sample.

A mercury arc lamp provided the broad-band source for cw fluorescence spectra, and a tungsten halogen lamp was used for broad-band excitation spectra. All narrow-band (<1 cm^{-1}) excitation spectra were taken with a high power pulsed nitrogen laser-pumped dye laser system. The cw fluorescence signals were dispersed with a Spex 1401 monochromator and detected photoelectrically. Because of the low signal levels, all time-resolved data required photon counting techniques.

III. MnF_2:Eu AND MnF_2:Er SYSTEMS

Some of the low-lying levels of Mn^{2+}, Eu^{3+}, and Er^{3+} are shown in Fig. 1. If the materials are optically pumped into the higher Mn^{2+} absorption bands, the Mn excitation rapidly relaxes to the lowest excited $^4T_1$ state. Below 4.2 K only the lowest $E1$ level of the $^4T_1$ state has a significant equilibrium population, and excitation transfer to the rare-earth ions will take place from this $E1$ level. It becomes important, then, to know which of the excited levels of the rare-earth ions are lower in energy than $E1$, or which, if any, might be in resonance with $E1$.

A. MnF_2:Eu spectroscopy

The $^5D_0$ level of Eu^{3+} is at 17266 cm^{-1}, which is 1157 cm^{-1} below the $E1$ level (18423 cm^{-1}). From

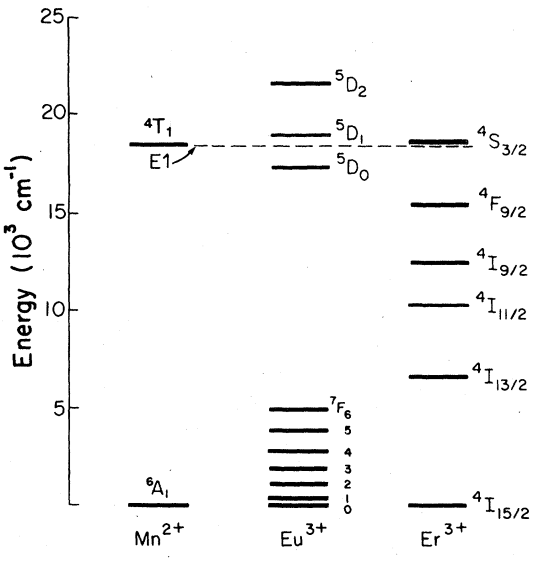

FIG. 1. Partial energy-level diagram for Mn^{2+}, Eu^{3+}, and Er^{3+}. The Stark splitting of the rare-earth levels is not shown, nor is the fine structure of Mn^{2+} levels. The $^4S_{3/2}$ level of Er^{3+} is shown higher in energy than the $E1$ level of Mn^{2+}. The measured separation between these levels is about 13 cm^{-1}.

their positions in other Eu^{3+} systems, we expect that the $^5D_1$ and $^5D_2$ levels will be approximately 600 and 3500 cm^{-1} above $E1$.[13,14] Using broad-band sources, we were unable to detect the Eu^{3+} absorption transitions in our crystal of MnF_2:Eu because of the very weak doping.

The fluorescence spectrum of MnF_2:Eu at 4.2 K is shown in Fig. 2. The narrow features at around 5500 Å and the broad band stretching from 5500– to 6500 Å are caused by emission from Mn traps. This part of the fluorescence is identical to the Mg-induced trap fluorescence seen in nominally pure MnF_2 crystals, where the trace amounts of Mg ions occur as unintentional impurities.[1] We see no evidence that doping the crystal with Eu ions causes the creation of new Mn traps.

The remaining sharp lines from 5790 Å upwards are identified as transitions from the $^5D_0$ state of Eu^{3+} to the various levels of the ^7F_J manifold. No fluorescence is observed from the $^5D_1$ and $^5D_2$ levels, even though in other Eu-doped materials strong fluorescence is observed from these levels.[11]

By monitoring one of the sharp Eu^{3+} lines while pumping the crystal with light of different wavelength, we were able to measure the Eu^{3+} excitation bands. In this experiment an incandescent lamp filtered through a quarter meter monochromator was used as an exciting source. The excitation bands were found to be identical with the

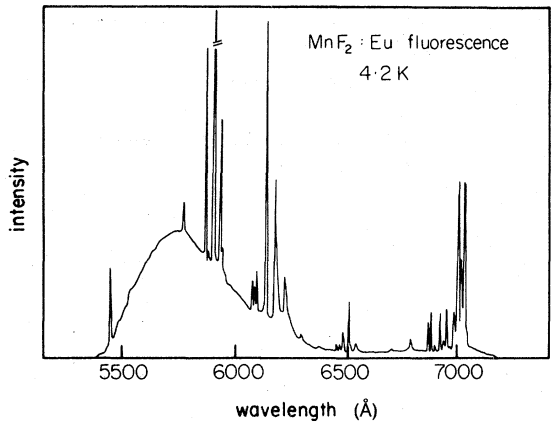

FIG. 2. Fluorescence spectrum of Mn F_2:Eu under broad-band excitation at 4.2 K. The sharp feature near 5500 Å and the broad continuum stretching from 5500 to 6500 Å originate on Mn ions. The single sharp line at 5790 Å is the $^5D_0 \rightarrow {}^7F_0$ transition, and the groups of lines to higher wavelengths are the transitions from $^5D_0$ to other ^7F_J levels.

Mn^{2+} absorption bands,[15] thereby confirming that the Eu^{3+} ions were pumped by energy transfer from this Mn^{2+} system. Direct excitation into the higher-lying Eu^{3+} levels was not observed in these experiments, due to the small number of Eu ions in the sample and to the weakness of the exciting light. An excitation experiment using a much more intense dye laser was used to find the $^5D_2$ level. It is interesting to note that on exciting the Eu^{3+} ions directly into the $^5D_2$ level, strong fluorescence was observed from the $^5D_0$ level. We did not find any comparable fluorescence from the $^5D_2$ and $^5D_1$ levels, although from experience with Eu^{3+} in diamagnetic hosts, one might expect a detectable fluorescence from at least one of these two levels. We believe that, when excited into the $^5D_2$ or $^5D_1$ level, the Eu ion relaxes by energy transfer to the $^4T_1$ state of one of the neighboring Mn ions, and this excited Mn ion in turn transfers its energy back to the lower $^5D_0$ level of the Eu^{3+} ion. Thus the presence of the Mn ions results in efficient nonradiative depopulation of the higher Eu levels and, as a result, fluorescence can only be observed from the $^5D_0$ level.

We note that Hirano and Shionoya in their study of $KMnF_3$:Eu^{3+} used Li as a charge-compensating agent and they report a 1-mol% doping with both Eu and Li.[9] This is a much higher dopant level than in our samples. Presumably, at this high Eu concentration, direct absorption into the higher Eu levels is an efficient excitation mechanism. Fluorescence from the $^5D_1$ level of Eu^{3+} was observed in this material even though the $^5D_1$ level is above the $E1$ of the Mn ion. In such heavily doped crystals, there is the possibility that, in addition to Eu ions substituting for Mn ions in the regular $KMnF_3$ lattice, some more complicated arrangements of Eu, Li, and Mn ions may also occur. If the coupling between Eu and Mn ions in such a complex is weaker than that for Eu ions in regular substitutional sites, then the fast relaxation of the Eu $^5D_1$ state through adjacent Mn ions may not be operative in this case. At 77 K the fluorescence from the Mn traps is quenched and only Eu fluorescence is observed. This facilitates a study of the spectroscopy of the Eu^{3+} ion in MnF_2.

The crystal field at the site of the Eu ion should cause a splitting of the $(2J+1)$-fold degenerate ^7F_J levels. For example, the $^5D_0 \rightarrow {}^7F_0$ transition should occur as a single line, and the $^5D_0 \rightarrow {}^7F_1$ transition should be split into three.

Radiative transitions between ^5D and ^7F states are forbidden by the spin selection rule, but this is relaxed by the spin-orbit interaction. Further, the Mn^{2+} site is one of inversion symmetry so we expect only magnetic dipole transitions for the ^5D-^7F transitions on Eu^{3+} ions which enter substitutionally for Mn^{2+}. The magnetic dipole J selection rule for $^5D_0 \rightarrow {}^7F_J$ is $\Delta J = 1$, hence only $^5D_0 \rightarrow {}^7F_1$ is allowed.

Although the $^5D_0 \rightarrow {}^7F_1$ transition is the strongest fluorescent feature, we also find fluorescence from $^5D_0$ to the other ^7F_J states. To check the dipole nature of all these transitions, we compared the spectra in α, σ, π polarizations (Fig. 3). The fluorescence patterns of $^5D_0 \rightarrow {}^7F_1$ are identical in π and α polarizations but are different from the σ polarization pattern, thereby indicating their magnetic dipole nature. All the other transitions have patterns which are similar in σ and α polarizations, indicating that they are electric dipole in character.

These details about the Eu fluorescence should enable us to draw some conclusions about the nature of the sites occupied by the Eu ions. We find that all the strong fluorescence lines have the same decay time at low temperatures, which would seem to imply that Eu^{3+} ions in one particular site are responsible for all the strong transitions. The substitution of Eu^{3+} for Mn^{2+} implies some mechanism of charge compensation. Different arrangements of local charge compensation might be expected to give rise to different Eu^{3+} site symmetries and, consequently, to a number of distinct Eu^{3+} centers. If this were so, then we would expect to see more than one line in the $^5D_0 \rightarrow {}^7F_0$ transition and more than three lines in the $^5D_0 \rightarrow {}^7F_1$ transition. We see only one $^5D_0 \rightarrow {}^7F_0$ line, and three strong lines are found for the $^5D_0 \rightarrow {}^7F_1$

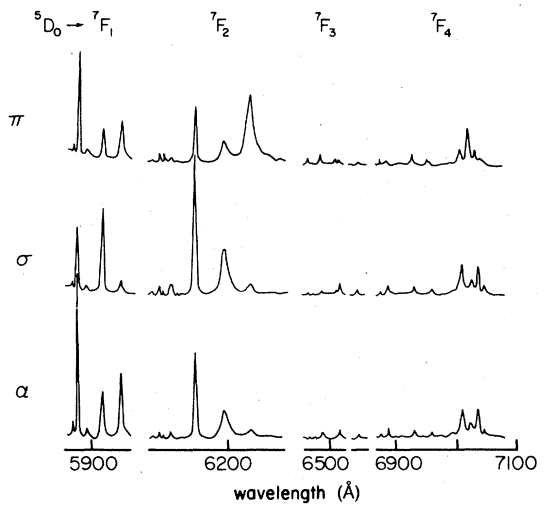

FIG. 3. Comparison of the π, σ, and α polarizations in the fluorescence spectrum of Mn F_2:Eu at 77 K. The similarity between the π and α patterns of the $^5D_0 \rightarrow {}^7F_1$ transitions and the dissimilarity of these with the σ pattern indicate that these are magnetic dipole transitions. The similarity of σ and α patterns for the other transitions indicate that they are predominantly electric dipole transitions.

transition, although some additional weak lines are also found in this transition (Fig. 3). These observations suggest that there is one predominant Eu^{3+} center. This could be (i) a center in which Eu^{3+} enters substitutionally for Mn^{2+} and no local charge compensation exists, or (ii) a center in which a specific form of local charge compensation occurs for each substitutional Eu^{3+} ion. We regard center (i) as the more likely, feeling that if local charge compensation exists, it is unlikely that all Eu^{3+} ions would experience an identical environment.

We attribute the occurrence of electric dipole transitions to minor distortions from perfect inversion symmetry which are due to strains, other impurities, or the effects of distant charge compensation.

In the MnF_2:Eu fluorescence spectrum seen at 4.2 K the Mn trap fluorescence is about five times as intense as the Eu fluorescence. The Mn traps are mainly Mn ions adjacent to Mg ions which should be present at concentrations of around 10 ppm. Each Mg ion will give rise to eight second-nearest neighbors and four third-nearest neighbors, each of which can act as a trap. The Eu concentration in the MnF_2:Eu crystal is 10 ppm. Hence the fivefold ratio of Mn trap fluorescence intensity to Eu fluorescence intensity is not unexpected.

We note, however, that in the experiments of Eremenko *et al.* on MnF_2:Eu,[7] a Eu concentration of around 0.1% ($\simeq$1000 ppm) was employed and in this material the Mn trap fluorescence was much more intense than the Eu fluorescence at low temperatures. Similarly, in their experiments on $KMnF_3$:Eu with Eu doping of 1 mol%, Hirano and Shionoya[9] show spectra taken at 4.2 K which indicate that the Mn trap fluorescence is again much more intense than the Eu fluorescence.

B. MnF_2:Er spectroscopy

When Er^{3+} substitutes for Mn^{2+} in MnF_2, the crystal field will remove all but the twofold Kramers degeneracy. Each $^S L_J$ state splits into $(2J+1)/2$ levels. The fluorescence spectrum from our highest-doped (400-ppm Er ions) crystal obtained by excitation in the blue using a mercury arc lamp is seen in Fig. 4. The sharp features at 5500 Å and the broad band stretching from 5500 to 6500 Å are due to fluorescence from Mn traps. From a study of the sharp structure of this fluorescence we find that the most strongly emitting traps are Mn ions which are adjacent to Mg and Zn impurity ions. We see no evidence of Er-induced traps.

The sharp features stretching from 6500-Å to higher wavelengths in Fig. 4 can be identified as fluorescence from the $^4F_{9/2}$ and lower Er levels. No fluorescence is observed from the $^4S_{3/2}$ state even though strong fluorescence is generally observed from this level of Er^{3+} in diamagnetic hosts when the material is pumped by blue exciting light.

The excitation bands of the Er^{3+} fluorescence were found from an excitation experiment using an incandescent lamp filtered through a quarter meter spectrometer as a pumping source. The excitation spectrum is identical to the Mn^{2+} absorption spectrum, indicating that in our samples the Er ions are being excited almost exclusively by energy transfer from Mn ions. Direct absorption into the higher-lying Er levels followed by luminescence from the lower Er levels is a much weaker process but can be detected when an intense tunable dye laser is used as an exciting source. The energy of the $^4S_{3/2}$ state was found in this way. It is about 13 cm^{-1} above the $E1$ exciton level, and one of its components overlaps the $E2$ absorption line. Since it is above $E1$, the $^4S_{3/2}$ level is not excited at low temperatures by energy transfer from Mn. This is consistent with the absence of fluorescence from the $^4S_{3/2}$ state in Fig. 4. Nor is fluorescence observed from $^4S_{3/2}$ when this state is excited directly by the dye laser. Instead, fluorescence is observed from the lower Er levels. This implies that a fast nonradiative relaxation occurs from $^4S_{3/2}$ to the lower Er levels in this system. We be-

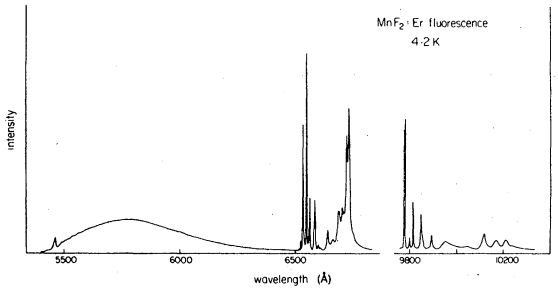

FIG. 4. Fluorescence spectrum of MnF_2:Er under broad band excitation at 4.2 K. The group of lines at around 6600 Å constitute the $^4F_{9/2} \rightarrow {}^4I_{15/2}$ transitions, while the $^4I_{11/2} \rightarrow {}^4I_{15/2}$ transitions are seen at around 1 μm. The $^4I_{13/2} \rightarrow {}^4I_{15/2}$ transitions occur at around 1.5 μm and are not shown here.

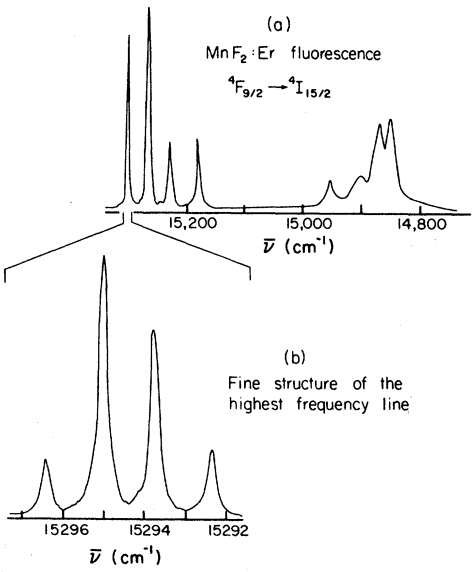

FIG. 5. Full eight-line pattern of the Er^{3+} $^4F_{9/2} \rightarrow {}^4I_{15/2}$ transition is shown in (a). Under high resolution the sharper lines are found to exhibit fine structure. The four-line fine-structure pattern of the highest-frequency line is shown in (b).

lieve that the excited $^4S_{3/2}$ state relaxes by energy transfer to a neighboring Mn ion, and this ion in turn transfers energy back to the lower levels of the Er ion. We do not feel that a direct phonon-assisted relaxation process in which $^4S_{3/2}$ decays by phonon emission to $^4F_{9/2}$ is responsible for the relaxation of the $^4S_{3/2}$ state in MnF_2:Er, since this is generally found to be a very weak process. The absence of fluorescence from the $^4S_{3/2}$ level of Er in MnF_2 was pointed out by Flaherty and Di Bartolo,[11] who also attribute it to the interaction with the neighboring Mn ions. They note in particular the overlap between the $^4S_{3/2}$ level and the $^4T_1$ absorption band of Mn.

The Er concentration in our most heavily doped MnF_2:Er crystal is 400 ppm, yet at helium temperatures the Mn trap fluorescence is about five times as intense as the $E1$ emission from the $^4F_{9/2}$ state, although the Mg, Zn, and Ca ions which are responsible for most of the Mn traps are believed to be present at a concentration of less than 100 ppm.

Figure 5 shows the fluorescence due to a transition between the lowest $^4F_{9/2}$ level and the $^4I_{15/2}$ ground state in a MnF_2:Er crystal with 16 ppm of Er ions. The crystal temperature was 2 K. We see the expected eight line pattern due to the crystal-field splitting of the $^4I_{15/2}$ ground state. Some weak additional lines were found in this transition in the more heavily doped (400 ppm) sample, and excitation experiments with the dye laser indicated that these additional lines originate on Er ions in different sites. Again, and for generally the same reasons as were advanced in discussing the Eu spectrum, we believe that the Er ions enter substitutionally into Mn sites without local charge compensation.

All of the Er lines observed either in fluorescence or in excitation that are adequately narrow show fine structure. This structure in the fluorescence transition between the lowest $^4F_{9/2}$ level and the lowest $^4I_{15/2}$ level, which is also seen in absorption (excitation) at low temperatures, is shown in Fig. 5. This line is split into four components approximately equally spaced. All four components have identical excitation spectra across the $^4I_{15/2} \rightarrow {}^4S_{3/2}$ region and consequently would seem to originate on the same Er ion; the splitting does not seem to be due to Er ions in different sites.

One intriguing possibility is that this fine structure is due to the lifting of the Kramers degeneracy by the internal exchange field. We have no experimental value of the Mn-Er exchange interactions, although we note that in a similar system—$KMnF_3$:Eu—the exchange interaction between Mn and Eu is strong enough to cause detectable magnon sidebands of one of the rare-earth transitions.[9]

IV. EXCITON DYNAMICS IN MnF_2 AND IN MnF_2 DOPED WITH RARE EARTHS

To investigate the competition between the transfer rates to the Mn traps and to the rare-earth ions, we can make a comparison between the feeding of the Mn traps in nominally pure samples and the feeding of both Mn traps and rare-earth ions in the rare-earth-doped samples. We begin with a discussion of the dynamics in the simpler nomin-

ally pure samples which do not suffer from the complication of simultaneous effects due to rare-earth impurities.

A. Exciton dynamics in nominally pure MnF_2 at low temperatures

Once $E1$ excitons are created, they can decay by three mechanisms: (i) radiative decay, (ii) biexciton decay, and (iii) transfer to traps. (We discount the possibility of efficient multiphonon relaxation across the 18420-cm^{-1} gap to the ground state.) The radiative decay rate is about 30 sec^{-1}, which is very small in comparison to the other processes. One consequence of this is a rather weak fluorescence in the $E1$ transition. The biexciton decay, which is characterized by a nonexponential time dependence, has been shown to be important at low temperatures and under intense pumping power.[16] Above 4 K, however, we find that transfer to the traps becomes the predominant decay mechanism. As evidence for this, the $E1$ decay becomes exponential above 4 K, and the decay rate increases rapidly with increasing temperature while the integrated fluorescence intensity from all Mn traps remains essentially constant (up to about 25 K). We interpret this as indicating that the efficient depopulation of the $E1$ exciton state above 4 K is due to a rapidly increasing transfer rate to the traps.

The relative constancy of the integrated fluorescence intensity over this temperature region provides some specific information about the nature of the traps that are being fed and about the radiative efficiency of the system. In addition to the fluorescing Mn traps, quenching traps also occur. We recall that when the temperature has reached 10 K, the second- and third-nearest-neighbor traps have ceased to be effective, only the deeper Mn traps and the quenching traps continue to be effective, and the excitation energy is now spread among these latter traps. The lack of any significant drop in the integrated fluorescence intensity over this temperature region, however, indicates that the quenching traps cannot compete successfully for the energy in the exciton state. Hence we conclude that, in our samples, the net transfer rate to the quenching traps is apparently much smaller than the transfer rate to the fluorescing Mn traps; the radiative efficiency of the excited Mn system is high.

A high radiative efficiency is also supported by the relaxation time measurements at low temperature. In a previous study of these pure MnF_2 crystals,[16] a net low-temperature transfer rate from $E1$ to all traps of about 8×10^3 sec^{-1} was inferred. The radiative decay rate from $E1$ is 30 sec^{-1}, indicating that the amount of excitation being transferred to traps is about 270 times that being radiated by the intrinsic exciton system. The observed ratio of trap to intrinsic fluorescence in these samples is measured to be ~250. Thus the fluorescing traps alone can account for the net transfer rate—the quenching traps do not participate significantly.

Our experiments make no statement about the absolute quantum efficiency of the material. What they do establish is that once an exciton is created, the probability that this energy will be emitted radiatively is high.

In the temperature range where the transfer to traps is the dominant decay mode of the $E1$ excitons, the transfer rate may be measured simply as the inverse of the exciton lifetime. The weak intrinsic fluorescence at $E1$ allows the exciton population to be monitored directly. The transfer rate $k(T)$ is seen to increase rapidly above 4 K. A semilog plot of $k(T)$ versus inverse temperature, shown in Fig. 6, indicates by the straight-line behavior that the increase with temperature follows a simple activation process.

It is important to realize that in many cases, and in particular in this case, it is possible to deter-

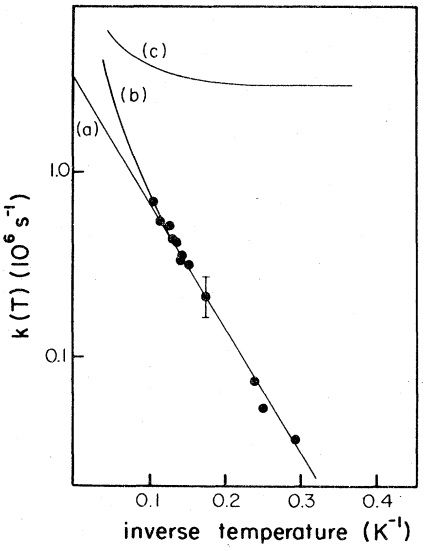

FIG. 6. Points show measured values of the decay rate of the intrinsic excitons between 3 and 10 K. The linear curve (a) is what is calculated for a setp-up process proceedings through a level 11.5 cm^{-1} above $E1$ and assuming a coupling strength, W, of 3×10^6 sec^{-1}. In this calculation the boson population function is approximated by a single exponential. Curve (*b*) is calculated for the same step-up process using the correct form of the boson population function. Curve (*c*) shows the calculated decay rate for a step-down process of the same coupling strength and energy gap.

mine whether the thermally activated process involves a step up or a step down in energy. The temperature dependence of the phonon-assisted (or magnon-assisted) rate for a step down in energy, $k_{ph}^{-}(T)$, is given by

$$k_{ph}^{-}(T) = W(1+n). \tag{1}$$

W is a measure of the coupling strength. n is the population of bosons with energy ΔE equal to the energy gap of the step, and varies with temperature as $n = [\exp(\Delta E/kT) - 1]^{-1}$. At $T = 0$, the step-down process has a residual rate equal to W.

The rate for a step-up process exhibits a similar activation behavior, but with no $T = 0$ residual rate:

$$k_{ph}^{+}(T) = Wn. \tag{2}$$

Taking into account other decay modes, designated as k_0, the net decay rate of the exciton state for a step-up or a step-down process becomes

$$k^{\pm}(T) = k_0 + k_{ph}^{\pm}(T). \tag{3}$$

At low temperatures, where $\Delta E/kT \gg 1$, the boson population n may be approximated by a simple exponential. The decay rate then satisfies the simple relationship

$$\ln|k(T) - k(0)| = \ln W - \Delta E/kT \tag{4}$$

for both step-up and step-down processes. Thus a semilog plot of the quantity $[k(T) - k(0)]$ against inverse temperature should be linear with slope $-\Delta E/k$ and intercept W in either case.

A vital difference remains, however, in the rate at $T = 0$, namely,

$$k(0) = \begin{cases} k_0 \text{ for a step-up process,} \\ k_0 + W \text{ for a step-down process} \end{cases}. \tag{5}$$

For a step-up process, $k(0)$ is merely the contribution from any thermally independent processes, and may be small in comparison to the intercept W. For a step-down process, however, $k(0)$ is necessarily at least as large as W. Thus the two processes may, in fact, be distinguished in many cases by the magnitude of the residual rate at $T = 0$. This is the quantity that must be subtracted from the raw data before the desired linearity is achieved.

In our experiments, after separation of the biexciton effects, the residual rate due to transfer and radiative decay was found to be $\sim 8 \times 10^3$ sec^{-1}. This is very small in comparison to the extrapolated high-temperature intercept read from Fig. 6 as $W = (3 \pm 1) \times 10^6$ sec^{-1}. Consequently, we may definitively attribute this activation behavior to a step-up process. For comparison, curve (*c*) of Fig. 6 shows the functional form for the decay rate for a step-down process of the same coupling strength and energy gap.

The magnitude of the energy gap is found from the slope of the best linear fit to the data to be $E = 11.5 \pm 2$ cm^{-1}. It should be noted that for this size energy gap, the approximation to the boson occupation number is already beginning to break down for the high-temperature data points. The correct functional form is indicated by curve (*b*) in Fig. 6. The small error introduced is hidden in the uncertainty in the data points.

Earlier work by Dietz *et al.* reported a similar exponential behavior, in that case in the decrease of the fluorescence intensity at $\sigma\dagger$. The magnitude of the energy barrier inferred from their data, however, is only 6.3 cm^{-1}.[17] We cannot explain this discrepancy satisfactorily, but suggest that it may be due to the difference in the quantities measured in the two experiments. For example, the thermal boil back of the shallower traps may affect the lifetime and intensity differently. Such boil back introduces a second exponential in the tail of our lifetime data, but this is easily deconvoluted from the early decay to give the desired transfer rate to the traps. Such deconvolution, however, is not possible in steady-state intensity measurements. Our lifetime data extend to 10 K only since, as the second-nearest-neighbor traps cease to be effective, the fluorescence is too weak and the decay too fast to accomplish this deconvolution.

We can interpret the activation behavior as indicating the existence of a level lying 11.5 ± 2 cm^{-1} above $E1$, out of which energy transfer to the traps occurs much more readily. This level could either be (i) a localized trap state near an impurity ion as suggested by Dietz *et al.*[17] or (ii) the intrinsic $E2$ state of the resonant ions.

As regards (i) we have seen that the effect on the $E1$ energy levels of Mn ions which are third-nearest neighbors to Mg on Zn impurities has been compared by Dietz to the effect of a [001] applied uniaxial stress. Since the pure electronic trap lines track exactly under [001] stress with the intrinsic $E1$ line, it may be feasible to extrapolate from the small externally applied stress to the large effective stresses induced locally by the impurities. Hence, from the depths of the 3nn traps it is possible to calculate the effective local "[001] stress" and thus the expected energy of the perturbed $E2$ excited states of these ions. From the data of Dietz *et al.*[24] this would give the $E2$ level of 3nn ions at about 12.5 cm^{-1} above the intrinsic $E1$ state, in good agreement with our activation energy. We have observed this activation, however, in the region of 3–10 K. Since it is known that 3nn Mn ions have ceased to be effective as traps by 5 K, it is unlikely that these sites can be responsible for the activation across this temper-

ature range. One could consider the role of 2nn Mn ions, but it is difficult to treat these on a uniaxial stress model.

On this model of activation to trap states, the activation occurs by tunneling from the exciton band to these strongly perturbed sites lying very close to the impurity ion. This represents a transfer of excitation between ions, however, which are only weakly coupled due to their large separation.

Some of these problems are resolved by considering the second possibility by which transfer takes place via a thermal activation to the intrinsic $E2$ state. The zone-center energy gap between the $E1$ and $E2$ exciton states is measured from the absorption spectrum to be 17 cm^{-1}.[3] Whereas $E1$ is believed to have a very small dispersion, a 6–7 cm^{-1} dispersion has been suggested for the $E2$ level,[18] which would bring the separation between $E1$ and $E2$ at zone edge into agreement with our activation result. We note however that Dietz *et al.*[17] have pointed out that their stress results can be interpreted as indicating a negligible dispersion for $E2$ as well as for $E1$. Even though the stress experiments indicate that the $E2$ dispersion is much less than 6 cm^{-1}, nevertheless, this model is self-consistent and gives some new physical insights concerning the exciton states.

Allowing for a 6–7-cm^{-1} negative dispersion for $E2$, the zone-boundary separation between $E1$ and $E2$ falls to 10–11 cm^{-1}. Our experimental results of 11.5 ± 2 cm^{-1} are then in good agreement with the $E1-E2$ energy gap at zone edge. It is also reasonable to assume that the activation at zone edge has a greater amplitude. The wave vector of an 11.5-cm^{-1} phonon (or magnon) will be quite small, resulting in an essentially vertical $E1-E2$ transition, as shown schematically in Fig. 7. Since the density of initial and final exciton states both peak close to the zone boundary, one would expect that transitions occurring at zone edge should predominate—provided that a substantial zone-edge population exists in the $E1$ (initial) state.

The population of $E1$ excitons at zone edge could conceivably depend both on the wave vector of the excitons initially created by the absorption process, and on the rate at which thermalization occurs across the Brillouin zone. For example, absorption at $E1$ results in an initial population of excitons clustered around $k = 0$. Dietz *et al.* have reported unequal decay rates of the fluorescence at $E1$ (zone-center excitons) and σ_1^* (zone-edge excitons).[19] This implies that thermalization does not occur even on a *ms* time scale. These data were taken on stressed samples at low pumping intensities.

On the other hand, results reported by Macfarlane and Luntz[20] on unstressed samples at high

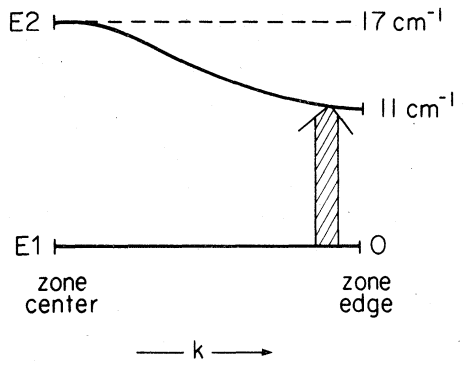

FIG. 7. In the presence of a negative dispersion of 6 cm^{-1} in the $E2$ exciton state, the gap between zone-edge exciton states of E_1 and $E2$ would be 11 cm^{-1}. Because of the greater density of exciton states at the zone edge, $E1 \rightarrow E2$ transitions should mainly occur across this 11-cm^{-1} band gap.

pump intensities indicate complete thermalization across the zone within a few μsec. Our data, taken under the same conditions, are consistent with these results. We see no discrepancy between the decay rates at $E1$ and σ_1^*. It is possible that the difference in conditions is responsible for the different thermalization times. At high pump intensities and zero stress, where the density and mobility of the excitons are much higher, exciton-exciton scattering may be an efficient mechanism for loss of phase memory. This hypothesis is supported by the linear dependence of the thermalization time on pumping power reported by Macfarlane and Luntz,[20] and by the substantial exciton-exciton interaction necessary for the biexciton decay rate observed under these conditions.[16]

These arguments indicate that thermalization is rapid in our experiments, and an $E1$ population should result that is heavily weighted towards zone edge, consistent with the density of states. Consequently, the thermal activation behavior should reflect the $E1-E2$ separation at zone edge rather than zone center. Our results are then consistent with a 5.5 ± 2-cm^{-1} negative dispersion for $E2$. We might note that a similar activation behavior is observed in the $E1$ fluorescence in $KMnF_3$, where the barrier is again about 5–6 cm^{-1} smaller than the zone-center separation between $E1$ and $E2$.[21]

It is also physically plausible that enhanced transfer to the traps would occur from the $E2$ exciton state. The homogeneous width of the metastable $E1$ state is expected to be extremely narrow, resulting in poor energy overlap between ions in slightly different crystalline environments. Of particular importance, transfer among ions whose $E1$ energy levels differ by only a fraction of

a wave number, such as at the periphery of the perturbation caused by an impurity ion, would be strongly inhibited. The narrow $E1$ states on neighboring ions would be slightly out of resonance, and transfer would necessarily be phonon assisted. The density of states of phonons with such small energies is vanishingly small, and a shell of many slightly perturbed Mn ions would present a sizable barrier in the transfer to the deeper traps.

Thermal activation to the $E2$ state could circumvent this bottleneck. Lying slightly above $E1$, $E2$ is lifetime broadened, due to the fast relaxation down to $E1$. Consequently energy in the $E2$ exciton state could be transferred resonantly among slightly perturbed Mn ions, allowing easier access to the deeper traps. Thus we conclude that thermal activation to the $E2$ state is both quantitatively consistent with the data and physically plausible.

With transfer to the traps taking place out of both $E1$ and $E2$ exciton states, as shown schematically in Fig. 8, we can express the net transfer rate as

$$k(T) = n_1(T)k_1 + n_2(T)k_2. \tag{6}$$

$n_1(T)$ and $n_2(T)$ represent the fractional populations of $E1$ and $E2$ exciton states, and k_1 and k_2 the coupling strengths of the respective exciton states to the localized trap states.

At low temperatures, only the $E1$ state is occupied, and the net transfer rate reduces to

$$k(T \to 0) = 1 \times k_1. \tag{7}$$

Thus the coupling strength to the $E1$ exciton state is equal to the net transfer rate at low temperatures, which was found to be $\sim 8 \times 10^3$ sec^{-1}. At higher temperatures the $E2$ state becomes thermally excited, eventually sharing the excited population equally with $E1$. Thus

$$k(T \gg \Delta E/k) \simeq \tfrac{1}{2}k_2 \tag{8}$$

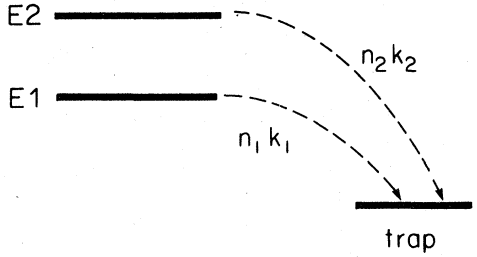

FIG. 8. Transfer rates, k_1 and k_2, from the $E1$ and $E2$ exciton states to the traps. n_1 and n_2 are the populations in the two exciton states.

and from the extrapolated high-temperature intercept, we obtain the coupling strength to the $E2$ exciton state, $k_2 = (6 \pm 2) \times 10^6$ sec^{-1}. A comparison of the two coupling strengths indicates that transfer to the traps occurs about a thousand times more readily out of the $E2$ exciton state. Note that a similar analysis can be adapted to the localized activation model. In that case k_1 and k_2 represent the matrix elements coupling the $E1$ exciton band to the perturbed $E1$ and $E2$ localized states, respectively.

A similar study was carried out in the Er^{3+}-doped samples, where the temperature dependence of the $E1$ decay rate was inferred from the feeding of the Er^{3+} ions. The results showed an activation behavior similar to that found in the pure samples, with no substantial differences in barrier height or coupling strengths.

B. Fluorescence behavior in nominally pure MnF_2 and in the rare-earth-doped MnF_2 at higher temperatures

We now look at the fluorescence behavior of the rare-earth-doped MnF_2 at higher temperatures and compare it with that found for nominally pure MnF_2. In Fig. 9 we plot the integrated Mn trap

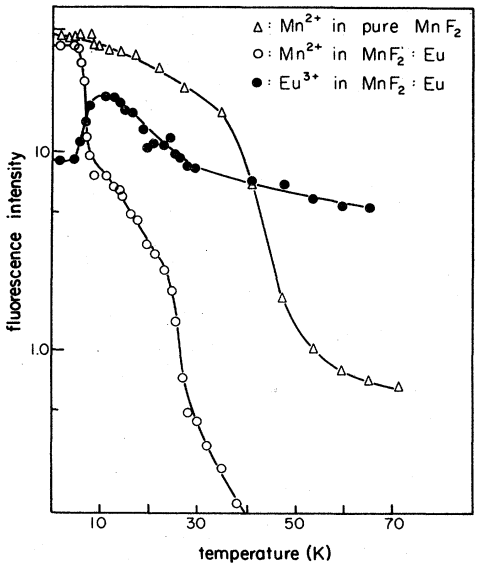

FIG. 9. Variation with increasing temperature of the fluorescence from Mn traps in nominally pure MnF_2, from Mn traps in MnF_2:Eu, and from Eu^{3+} ions in MnF_2:Eu. The same intensity scale is used to describe both the Mn trap and the Eu^{3+} fluorescence from MnF_2:Eu, and at low temperatures the Eu^{3+} fluorescence is about one fifth as intense as the Mn trap fluoresence. The intensity scale for the fluorescence intensity from nominally pure MnF_2 was selected arbitrarily.

intensity as a function of temperature for nominally pure MnF_2 and for MnF_2:Eu. There is little change in the intensity of the pure sample up to 30 K, even though the spectrum shifts to the red by about 300 cm^{-1} between 8 and 10 K. In MnF_2:Eu, on the other hand, there is an order-of-magnitude decrease in the integrated Mn trap fluorescence intensity between 8 and 10 K which is accompanied by a threefold rise in the Eu intensity.

A similar result is found for MnF_2:Er. Intensity measurements on one of the samples (that with 400-ppm Er) show that there is a sudden order-of-magnitude decrease in the integrated Mn trap fluorescence at around 10–11 K with a more gradual rise in the Er fluorescence intensity. We address ourselves to the origin of these intensity variations in Sec. IV C.

As Fig. 9 shows, in MnF_2:Eu the Eu fluorescence intensity remains approximately constant between 30 and 70 K, above which it decreases rapidly with increasing temperature. Figure 10 shows that the intensity I varies as

$$1/I = c_1 \exp(-\Delta/kT) + c_2. \tag{9}$$

This is the behavior expected from a model in which the Eu ions lose their excitation by boil back to the regular Mn ions, and this energy is transferred via the $E1$ excitons to the quenching traps.[1] The value of Δ from the data of Fig. 10 is 1350 cm^{-1} which is about 200 cm^{-1} larger than the gap between the $^5D_0$ level of Eu^{3+} and the $E1$ level of Mn^{2+}.

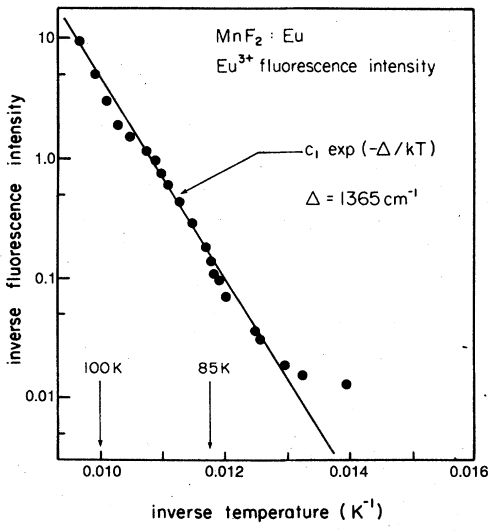

FIG. 10. Variation with temperature of the intensity (I) of the Eu^{3+} fluorescence from MnF_2:Eu. The predicted behavior is $1/I = c_1 \exp(-\Delta/kT) + c_2$.

This same model would predict a relaxation rate ($1/\tau$) for the Eu luminescence given by

$$1/\tau = c \exp(-\Delta/kT) + 1/\tau_R, \tag{10}$$

where τ_R is the decay time at very low temperatures—presumably purely radiative. $\tau_R = 9$ msec. The observed decay rate follows this pattern, with $\Delta = 1225$ cm^{-1}, still somewhat larger than the separation between $E1$ and $^5D_0$. We believe that this model explains the behavior of the Eu fluorescence in the higher-temperature (~100 K) region. The fact that the value of Δ is somewhat larger than the 1150-cm^{-1} gap between the $^5D_0$ and $E1$ electronic levels may be caused by the boil back process going from the $^5D_0$ electronic level of Eu to a higher vibrational level associated with the $E1$ state of Mn.

Since the fluorescence levels of Er are more than 3000 cm^{-1} below E1, Er traps remain effective at much higher temperatures and their fluorescence can still be observed from MnF_2:Er at room temperature.

C. Nature and effectiveness of the Mn traps

In this section we inquire a little further into the nature of the Mn traps and attempt to explain the low-temperature intensity behavior of the rare-earth-doped MnF_2 crystals such as that seen in Fig. 9.

The Mn traps which are most effective at low temperatures are Mn ions which occur as second- and third-nearest neighbors (2nn and 3nn) to Mg and/or Zn ions. In addition, some deeper Mn traps become effective at higher temperatures. These are Mn ions which are more strongly perturbed by defects and impurities. Mn ions which occur as first-nearest neighbors (1nn) to Ca^{2+} ions have been identified as one such type of deep trap.[1] This identification was possible because these Ca-perturbed Mn ions emit a sharp identifiable no-phonon no-magnon line.

Similar sharp fluorescence lines from Mn ions in 1nn sites around Mg or Zn ions have not been found. As discussed earlier, Mg(1nn) and Zn(1nn) may not in fact be deep traps, or simply do not give rise to sharp line emission.

The feeding of the traps occurs by excitation transfer along chains of adjacent Mn ions. Now, although the $E1$ level of the 2nn Mn ions is below that of the 3nn ion, the excitation on the 3nn is not transferred to 2nn. Both can act as traps. The reason for this is that the excitations can move readily between Mn ions *on the same sublattice*, but transfer between adjacent ions on opposite sublattices is a much less probable process,[22] and does not occur within the exciton lifetime.[17]

Around each substitutional Mg or Zn ion the 2nn Mn ions are the most numerous trap species, and there are no other effective Mn traps on the sublattice which contains these 2nn ions. Hence we might expect that 2nn ions would play a more active role as traps than either 3nn or 1nn ions. Such is found experimentally; at 1.5 K, where 2nn and 3nn are both effective, the fluorescence intensity from 2nn ions is observed to be about four times as strong as that from 3nn ions, and from the extent of the spectral change in the Mn trap fluorescence between 8 and 10 K, we infer that below 8 K the 2nn fluorescence is much stronger than that of the 1nn ions.

Between 3 and 5 K the 3nn Mn traps lose their energy by boil back. And between 8 and 10 K the 2nn Mn traps lose their effectiveness. Now if the concentration of traps other than Mn traps is small, the excitation boiled off from the 2nn traps will go mainly to the deeper Mn traps with little change in integrated fluorescence intensity. This is what we observe in the case of the flourescence from nominally pure MnF_2 crystals (Fig. 9).

If, however, Eu or Er ions are present in the crystal, then at low temperatures they must compete with the 1nn, 2nn, and 3nn Mn ions for the energy pumped into the MnF_2 exciton system. If the concentration of rare-earth ions is small, as is the case here, the ratio of rare-earth to Mn flourescence will be low. Between 8 and 10 K, however, where the efficient 2nn traps lose their effectiveness, the energy lost by the 2nn traps will be shared between the 1nn ions and the Eu or Er ions. Hence, with appropriately small rare-earth doping, we would expect to see a decrease in Mn trap fluorescence with a concomitant rise in the rare-earth fluorescence between 8 and 10 K. This may explain the changes in the Mn and Eu flourescences between 8 and 10 K which are seen in Fig. 9, and may explain the similar behavior seen in the MnF_2:Er sample.

Another possible explanation for these changes in the fluorescence ratio could be the occurrence of an impediment to the Mn → rare-earth transfer at low temperatures, which is removed at higher temperatures. Such an impediment could be a barrier, caused by the Mn ions near the rare-earth ion having their $E1$ levels *higher* in energy than the regular Mn ions.[23] This could act as an effective barrier at low temperatures, but at higher temperatures thermal phonons will permit this barrier to be overcome.

We attempted to find evidence for such a barrier in MnF_2:Er by exciting the $^4S_{3/2}$ level of Er directly with a tunable dye laser pulse at 2 K. If the nearest Mn ion has its $E1$ level higher in energy than that of the regular Mn ions (Fig. 11), then

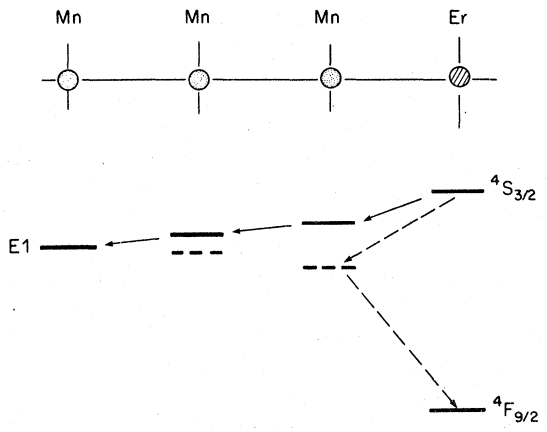

FIG. 11. Full arrows denote the most probable excitation transfer path in the case where the $E1$ energy levels of the Mn ions adjacent to the Er ion are higher in energy than the $E1$ levels of the regular Mn ions. The most probable excitation transfer path in the case where the adjacent ions are lower in energy is indicated by the broken arrows.

we expect that the excitation in the $^4S_{3/2}$ state will be transmitted to this nearby Mn ion and will then be transferred to the regular Mn ions for transfer to Mn traps or other Er ions. This process is indicated by the full arrows in Fig. 11. We would expect some of this energy to end up as Mn trap flourescence. If, on the other hand, the nearby Mn ion is lower in energy than the regular Mn ions, then the $^4S_{3/2}$ level will transfer its energy first to this nearby Mn ion, after which it is transferred back to the $^4F_{9/2}$ level of the Er ion (broken arrows in Fig. 11). Only Er luminescence should be observed in this case.

An excitation experiment was carried out to check this point. The exciting laser light was tuned across a frequency band containing one of the $^4S_{3/2}$ absorption lines. There was no change in the background Mn fluorescence intensity as the laser frequency was tuned across this band. An additional Er fluorescence (from the $^4F_{9/2}$ and lower levels) was found, however, when the laser frequency coincided with the Er $^4S_{3/2}$ absorption. This experiment seems to militate against the barrier model in the MnF_2:Er case. Presumably a similar barrier does not occur in the MnF_2:Eu case, either.

The most likely explanation for the changes in intensity found in the 8–11 K temperature regions would then seem to be the elimination of the very effective second-nearest-neighbor Mn traps with, as a result, a much greater share of the excitation going to the rare-earth ions.

V. CONCLUSIONS

MnF_2 is regarded as a good test system to examine, among other things, the optical properties of magnetic insulators. In this paper we have examined the flourescence from nominally pure MnF_2 and from MnF_2 doped with trace amounts of Eu and Er ions. In particular, we were interested in studying the energy transfer and exciton decay processes in the pure and rare-earth-doped materials.

The exciton transfer rate increases rapidly with increasing temperature, suggesting that a much more effective transfer to traps by a thermal activation to an intrinsic or localized $E2$ state. In the materials containing trace amounts of Eu and Er, the rare-earth ions are excited mainly by transfer from the regular Mn ions and must compete with the Mn traps for the excitation. As some of the Mn traps become thermally deactivated, the excitation energy redistributes itself among the remaining traps, and this leads to temperature-dependent variations in the fluorescence spectra of the doped materials.

There are some discrepancies which we are unable to resolve between our results and those of some previous workers. These discrepancies are pointed out in the paper. It is clear that there is need for further work on this very interesting material.

ACKNOWLEDGMENT

We would like to thank R. E. Dietz for many helpful discussions and for letting us see some of his unpublished data. Work for this paper was supported by the NSF under Grant No. DMR76-21574 and by the Irish National Science Council under Grant No. URG/18/77.

---

*Present address: Bell Laboratories, Murray Hill, N. J. 07974.
†Present address: Dept. of Phys., Univ. of Wisconsin, Madison, Wisc. 53706.

[1]R. L. Greene, D. D. Sell, R. S. Feigelson, G. F. Imbusch and H. J. Guggenheim, Phys. Rev. 171, 600 (1968).
[2]R. E. Dietz and A. Misetich, *Localized Excitations in Solids* (Plenum, New York, 1968), p. 366; A. Misetich, R. E. Dietz, and H. J. Guggenheim, *ibid.* p. 379.
[3]D. D. Sell, R. L. Greene, and R. M. White, Phys. Rev. 158, 489 (1967).
[4]We use the label Mg(2nn) instead of Mg(II) which was used previously (e.g. Ref. 1) to avoid confusion with the labeling used to describe oxidation states.
[5]J. M. Flaherty and B. Di Bartolo, Phys. Rev. B 8, 5232 (1973).
[6]K. Gooen, B. Di Bartolo, M. Alam, R. C. Powell, and A. Linz, Phys. Rev. 177, 615 (1969).
[7]V. V. Eremenko, E. V. Matyushkin, and S. V. Petrov, Phys. Status Solidi 18, 683 (1966).
[8]V. V. Eremenko and E. V. Matyushkin, Opt. Spectrosc. 23, 234 (1967).
[9]M. Hirano and S. Shionoya, J. Phys. Soc. Jpn. 28, 926 (1970).
[10]S. Shionoya and M. Hirano, Phys. Lett. A 26, 533 (1968).
[11]J. M. Flaherty and B. Di Bartolo, J. Lumin. 8, 51 (1973).
[12]E. V. Matyushkin, L. S. Kukushkin, and V. V. Eremenko, Phys. Status Solidi 22, 65 (1967).
[13]L. G. De Shazer and G. H. Dieke, J. Chem. Phys. 38, 2190 (1963).
[14]N. C. Chang and J. B. Gruber, J. Chem. Phys. 41, 3227 (1964).
[15]J. W. Stout, J. Chem. Phys. 31, 709 (1959).
[16]B. A. Wilson, J. Hegarty, and W. W. Yen, Phys. Rev. Lett. 41, 268 (1978).
[17]R. E. Dietz, A. E. Meixner, H. J. Guggenheim, and A. Misetich, J. Lumin. 1,2, 279 (1970).
[18]N. M. Amer, J. C. Chiang, and Y. R. Shen, Phys. Rev. Lett. 34, 1454 (1975).
[19]R. E. Dietz, A. E. Meixner, H. J. Guggenheim, and A. Misetich, Phys. Rev. Lett. 21, 1067 (1968).
[20]R. M. Macfarlane and A. D. Luntz, Phys. Rev. Lett. 31, 832 (1975).
[21]E. Strauss (private communication).
[22]J. F. Holzrichter, R. M. Macfarlane, and A. L. Schawlow, Phys. Rev. Lett. 26, 652 (1971).
[23]J. Hegarty and G. F. Imbusch, Colloq. Int. C. N. R. S. 255, 199 (1977).
[24]R. E. Deitz, A. Misetich, and H. J. Guggenheim, Phys. Rev. Lett. 16, 841 (1966).
[25]R. E. Deitz (private communication).